

## Interferometric Techniques for Magnetic Resonance Imaging

K. O. Johnson<sup>1</sup>, and C. H. Meyer<sup>1</sup>

<sup>1</sup>Biomedical Engineering, University of Virginia, Charlottesville, VA, United States

**Introduction:** Interferometry is a powerful method of imaging for various fields, such as radio astronomy [1, 2] and microscopy. Direct application of spatial interferometry for NMR and MRI has been rejected due to the distances necessary ( $\sim 10^8$  m) between receiver elements [3]. This work presents the application of interferometric techniques using a single receiver element. Spectroscopic imaging provides a platform for immediate application of this idea.

**Theory:** 2-D Spectroscopic imaging collects temporal k-space readouts,  $S(\mathbf{k}, t)$ , of an image,  $s(\mathbf{r}, f)$ . The data from two different k-space locations can be cross-correlated temporally to produce the mutual coherence function,  $G(\mathbf{k}_1, \mathbf{k}_2, t')$ .

$$G(\mathbf{k}_1, \mathbf{k}_2, t') = \int S(\mathbf{k}_1, t) S^*(\mathbf{k}_2, t - t') dt \quad (1)$$

By application of the van Cittert-Zernike theorem and the Wiener-Khinchin theorem, the mutual coherence function is equivalent to the Fourier transform of the image squared (for a derivation see Chapter 14 of [1]).

$$G(\mathbf{k}', t') = \iint |s(\mathbf{r}, f)|^2 e^{j\mathbf{r}\cdot\mathbf{k}'} e^{-j t' f} d\mathbf{r} df \quad (2)$$

Rather than mapping the coherence function to the relative positions of receiver elements (as in radio astronomy), Eq. (2) is dependent on the relative difference in the k-space locations of two signals where  $\mathbf{k}' = \mathbf{k}_1 - \mathbf{k}_2$ . Therefore the mutual coherence function provides an alternative method of acquiring MR

image data. Strictly, the van Cittert-Zernike theorem applies to spatially incoherent sources. MR spectra can be regarded as a quasi-monochromatic source. The information from sufficiently long readout times of a quasi-monochromatic source (readout longer than one over the spectral linewidth) will not behave in a coherent manner, allowing the application of interferometry [4]. The image phase is lost when correlating two signals to produce the mutual coherence function. Higher order correlations, such as the triple-correlation, are capable of preserving phase [5].

**Methods and Results:** Phantom data were collected for a 12x12 MR spectroscopic image. The phantom consisted of a bottle of oil placed next to a water cylinder (the excitation pulse cuts off the right side of the phantom). An ensemble average was taken over the repetitions of each possible  $\mathbf{k}'$ , decreasing possible coherence artifacts. Images resulting from the correlation are presented in Figs. 1 and 2 along with images from the conventional reconstruction (inverse Fourier transform of  $S$ ). Fourier inversion causes the sidelobes of the sinc to spread signal from one voxel into nearby voxels inversely proportional to distance (referred to as streaking here). A square root after Fourier inversion will spread the signal inversely proportional to the square root of the distance. While the correlation image  $|FT^{-1}\{G(\mathbf{k}', t')\}|$  is relatively artifact free in Fig. 1 (b), streaking corrupts the magnitude of the spectra  $|FT^{-1}\{G(\mathbf{k}', t')\}|^{1/2} \sim |s(\mathbf{r}, f)|$  for the correlation image in Fig. 2 (b). The magnitude of the spectra from two image locations (the locations of peak lipid and water signal) are plotted in Fig. 3 for both reconstructions. In the lipid spectra, water contamination is more evident in the correlation image, Fig. 3 (b), as compared to the conventional reconstruction.

**Discussion:** There are two immediate benefits of the proposed technique. Because each readout is correlated with every other readout,  $N$  readouts can maximally produce  $N(N-1)$  locations of  $G(\mathbf{k}', t')$ . This property will reduce the number of readouts required and will drive new acquisition strategies.

Another immediate benefit is enhanced resolution, illustrated in Fig. 1 (b), as  $\max |\mathbf{k}'| = 2\max |\mathbf{k}|$  for symmetric k-space data. Straightforward inversion of the correlation (Fourier transform followed by a square root) results in considerable image streaking, which decays with  $|\mathbf{r}|^{-1/2}$ . Future work would include a constrained or non-linear reconstruction method to mitigate the streaking. Significant developments are necessary to refine the proposed technique, both in acquisition and reconstruction. Application of interferometry to MR imaging will provide new methods of acquisition, reconstruction and analysis that may extend beyond spectroscopic imaging. This preliminary study has demonstrated some immediate benefits of the application of interferometry.

**References:** [1] Thompson, Moran and Swenson. 2001. *Interferometry and Synthesis in Radio Astronomy*. Second. Wiley-VCH. [2] Swenson and Mathur. 1968. The interferometer in radio astronomy. *Proc. of the IEEE* 56: 2114-2130. [3] Ernst, Richard R. 1992. Nuclear Magnetic Resonance Fourier Transform Spectroscopy (Nobel Lecture). *Angewandte Chemie International Edition in English* 31: 805-823. [4] Beran and Parent. 1974. *Theory of partial coherence*. Second. Society of Photo-optical Instrumentation Engineers. [5] Lohmann, Weigelt and Wirtzner. 1983. Speckle masking in astronomy:

triple correlation theory and applications. *Applied Optics* 22: 4028-4037.

**Acknowledgements:** NIH R01HL079110, NIH T32HL007284, Siemens Medical Solutions.

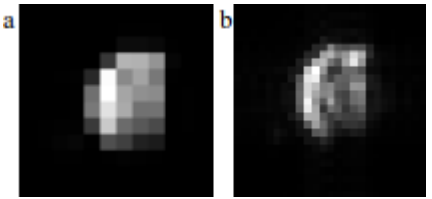


Figure 1: Images created by summing the power spectra. Source data were taken from the conventional reconstruction (a) and the proposed technique (b). The interferometric reconstruction provides enhanced resolution.

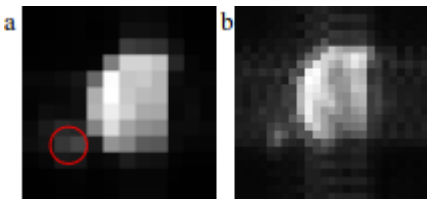


Figure 2: Images created by summing the absolute spectra. Each image corresponds to Fig. 1, summed over a square root. Source data are taken from conventional reconstruction (a) and the proposed technique (b). While benefiting from improved spatial resolution, the interferometric reconstruction (b) suffers from considerable streaking. Circled in red is the approximate position of the lipid bottle.

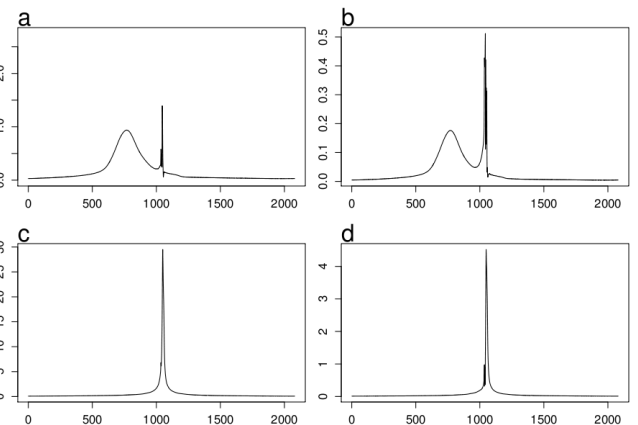


Figure 3: Spectra of a lipid signal (a, b) and a water signal (c, d) using the conventional reconstruction (a, c) and using the proposed technique (b, d). Streaking of water signal is evident in both (a) and (b), however it is much stronger for the correlation data (b).